

Chapter 4

Screening mechanisms on mixed C_{60} /TPC films

This chapter focuses on the study of both the structural and electronic properties of mixed structures built from the combination of C_{60} and TPC. Even though the structure of supramolecular architectures formed by the mixed growth of C_{60} with different types of hydrocarbons have been characterized during the last years [67, 68, 69, 70], it is only very recently that the study of the electronic properties associated to the C_{60} embedded in such molecular networks has commenced [71, 72, 73]. In our case, the various self-organized patterns obtained from different preparation conditions (ratio of molecules and surface temperature during molecular deposition) provide a good scenario to explore the role that a polarizable neighborhood plays on the electronic properties of a single molecule.

4.0.1 Screening and energy level alignment

When a charged particle is placed or removed from a neutral molecule, additional energy U due to the Coulomb repulsion/attraction with other charges embedded in the molecule has to be given. This is known as the on-site Hubbard energy. It modifies the molecular levels resulting in a HOMO-LUMO distance larger than in a simple "one-particle" scenario [74]. In the case of a free molecule the real molecule gap¹ is given by the difference between the ionization potential (IP) and the electron affinity (EA). These levels are sharp in energy and well localized. The energy difference among them, i.e., the $(E_{IP}-E_{EA})$ gap, is the energy $2U + \Delta$, where U is the Hubbard energy and Δ the gap in the one-particle scenario.

When the molecule is in contact with a surface or in a molecular self-assembled system, the value of the molecular gap changes due to the screening of mobile charge carriers in the electronic environment. Such electric screening reduces the value of U .

There are two main screening mechanisms for a molecule adsorbed on a surface: i) screening from neighboring molecules on a self-assembled molecular structure, and ii) screening from charges on a metal surface. Both mechanisms are sketched in Fig. 4.1.

The first screening mechanism is related to the polarizability of the surrounding molecules. Under the action of an applied field, the electrons are able to redistribute

¹Energy difference between the anionic and cationic ground states.

along the molecular cage [75]. This effect reduces the charging energy U by a factor of [76]

$$N \times f(\alpha) = \frac{Ne^2\alpha}{2R^4} \quad (4.1)$$

where α is the molecular polarizability, R the inter-molecular distance and N the coordination number, i.e, the number of neighboring charges. As it can be deduced from the equation, the stabilization of the charge 'reorganization' inside a molecule decreases strongly ($\sim 1/R^4$) with the distance from the charge center. It is then a short-range interaction that actuates only when the molecules interact forming densely packed bulk structures or a bi-dimensional film.

The second screening mechanism implies charge redistribution at the metal-molecule interface. The charging of a molecule located at the interface creates an image charge at the surface. The interaction between both the charged molecule and image charge reduces the ionization potential and increases the electron affinity by

$$E_i = \frac{e^2}{2D} \quad (4.2)$$

where D is the distance between the molecule and the created charge at the surface [77].

Besides U reduction, additional effects caused by the interaction between the molecule and the underlying surface are broadening and possibly degeneracy splitting of molecular resonances due to chemisorptive interaction and symmetry breaking, respectively.

In this chapter we evaluate the effect of the above described screening mechanisms using C₆₀ [78] as a probe molecule. The election of C₆₀ is based on its electronic configuration, which is maintained fairly unperturbed upon adsorption. Due to its symmetry, molecular orbitals are largely degenerated. In particular HOMO and LUMO have degeneracies 5 and 3, respectively, making these orbitals easy to detect by spectroscopic techniques. We take the lineshape and alignment of the LUMO and the HOMO-LUMO molecular bandgap as fingerprints of the local electronic properties. The screening is studied in three different situations: C₆₀ embedded in a pure fullerene island, isolated C₆₀, and C₆₀ mixed with the hydrocarbon TPC, whose properties have been described in the previous chapter. In order to obtain the individual or self-assembled molecular structures we deposit them at different surface temperatures and molecular ratio (in the case of the mixed self-assembled systems).

We use a Au(111) surface as a metal substrate throughout all the study. In this way, energy level alignment can be qualitatively compared between the different systems explored.

4.0.2 Polarizability of C₆₀ adsorbed on Au(111)

Fullerene adsorption on Au surfaces has been extensively studied during the last years, producing a wealthy amount of information about structural phases [49, 79, 80, 81, 82] and their electronic configurations [49, 83, 84, 85, 86, 87, 88]. Charge transfer on Au(111) is fairly small, as observed by STS and DFT calculations [85, 89]. The LUMO resonance of C₆₀ adsorbed on Au(111) lies far away from the Fermi level; therefore it is

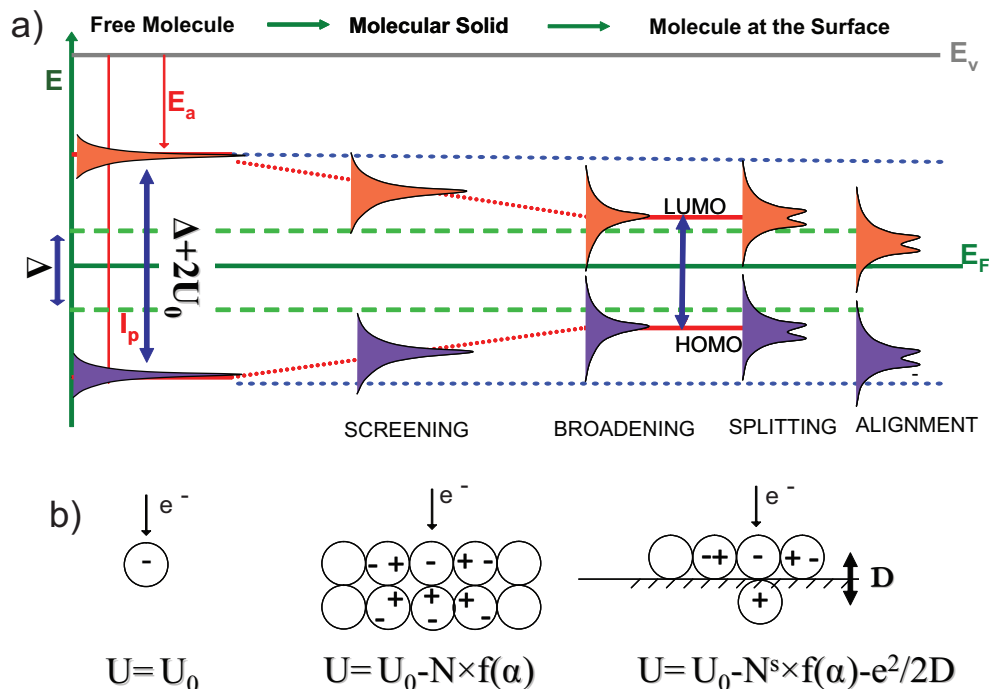


Figure 4.1: (a) Drawing of the molecular energy level alignment and the reduction of the on-site Hubbard energy, U , due to screening by neighboring molecules and by the surface. Δ represents the gap of the neutral molecule. Interaction with a metal can also add broadening and degeneracy splitting due to chemisorption. (b) Variation of the Hubbard energy U in the different molecular and metals scenarios.

expected that small changes in its alignment will not alter significantly the electronic character of the molecule, allowing us to interpret level shifts as only due to screening effects from the underlying surface and the molecular environment.

Upon deposition on a room temperature Au(111) surface, fullerene molecules diffuse and form bi-dimensional islands with hexagonal symmetry (Fig. 4.2(a)). Such island growth is driven by weak van der Waals interactions with an average intermolecular distance of 10 Å. The self-assembled structures are commensurated with the underlying Au(111) surface and the C_{60} molecules are adsorbed following different orientations [49]. STS measurements performed on single molecules embedded in the pure islands, i.e., surrounded by six neighbors, show two features around the Fermi energy that can be related to the alignment of molecular frontier resonances (Fig. 4.2(d)). At positive sample bias, i.e. probing the unoccupied DOS of molecule/surface, the peak located at 0.7 eV is associated with the LUMO derived resonance with a linewidth of typically 0.5 eV full width half maximum (FWHM). At negative sample bias we find the HOMO derived resonance located around 1.7 eV below the Fermi level (Fig. 4.2(d)). It appears usually like a shoulder. At negative sample bias the STS are dominated by the tip's

unoccupied structure being, in some cases, the spectroscopy fingerprints not so well defined as in the case of unoccupied levels. The HOMO-LUMO distance reveals a gap of 2.4 ± 0.1 eV, consistent with the values described in the literature [49, 83].

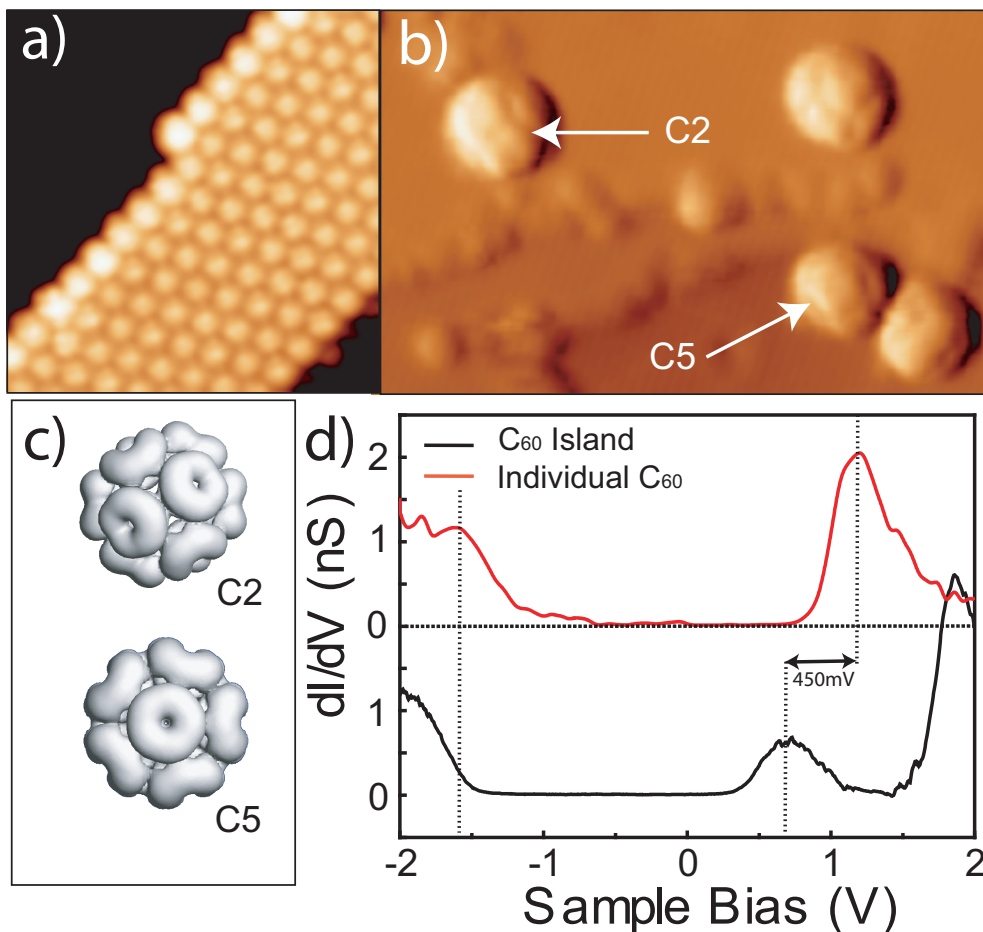


Figure 4.2: (a) Hexagonal self-assembled phase of C_{60} deposited on Au(111) at 300 K ($V = -1$ V, $I = 0.86$ nA). (b) Individual fullerene molecules deposited on a cold (80K) Au(111) surface. Different molecular orientations can be resolved in the intramolecular structure ($V = 2$ V, $I = 0.13$ nA). (c) Calculated isosurfaces of constant density of states for the LUMO orbital of a free C_{60} molecule, showing the symmetry axis C2 and C5. The lobes correspond to the DOS accumulation on the pentagonal faces of the C_{60} cage [90]. (d) STS spectra obtained on the self-assembled C_{60} island (bottom plot) ($V = 2.5$ V, $I = 1.9$ nA) and onto individual fullerenes (top plot) ($V = 2$ V, $I = 1.1$ nA). The difference in the gap amounts ~ 400 meV.

These result evidences a HOMO-LUMO gap reduction compared to the gas phase value, 4.95 eV², and the bulk gap, 3.3 eV [96], whose origin can only be attributed to

²value defined as the difference between the ionization potential (IP = 7.6 eV) [91, 92, 93, 94] and the electron affinity (EA = 2.65 eV) [95]

a strong screening produced by the molecular neighborhood and the metal substrate.

In order to give a quantitative estimation for the molecular screening, we compare the spectra obtained in the self-assembled hexagonal phase with that on individual C_{60} (Fig. 4.2(b)). To obtain isolated molecules we sublime them onto a cold (80 K) surface. At that temperature the molecular lateral diffusion is frozen, thus hindering the self-assembling in organized structures. Intra-molecular resolution allows to distinguish C_{60} adsorption along different orientations (Fig. 4.2(b) and corresponding calculated isosurfaces (c)). STS measurements performed on single C_{60} molecules located away from step edges show a LUMO derived resonance at typically 1.1 eV. The linewidth associated to the peak is similar to the self-assembled case, around 0.5 eV FWHM (Fig. 4.2(d)). The HOMO-LUMO gap is larger amounting to a value of 2.8 ± 0.1 eV. We associate this increase in energy gap of ~ 400 meV to the removal of the six C_{60} neighbors. To quantify the screening effect of each fullerene we apply Eq. 4.1 with intermolecular distance $R = 10 \text{ \AA}$ and polarizability $\alpha = 90 \text{ \AA}^3$ [76]. According to this relation, the interaction of each fullerene in the proximity accounts to a reduction of the Coulomb charging energy of 65 meV. For the case of $N = 6$ neighbors the change of U of $6 \times 65 \text{ meV} = 390 \text{ meV}$ obtained from this simple approach accounts closely to the experimental HOMO-LUMO gap increase.

4.1 Co-adsorption of C_{60} and triptycene on Au(111)

The role of the screening on the molecular level alignment can be further explored by changing the polarizability of the molecular environment, i.e., by embedding C_{60} in a molecular network with different electronic properties. An appropriate choice for that purpose is TPC (Fig. 4.3(a)). As described in the previous chapter, TPC consists of three phenyl moieties arranged in a rotor shape that makes this molecule a good candidate to form an inclusion complex with the spherical cage of the C_{60} molecule (Fig. 4.3(b)) via $\pi - \pi$ interactions (Fig. 4.3(c)). This has been observed in the bulk structure of TPC/ C_{60} molecular crystals [10, 11, 97]. The formation of the inclusion complex at the surface will be favored by the weak physisorption state of TPC on Au(111). The intermolecular interactions are expected to be stronger than adsorption and, consequently, it is more favorable for TPC to face the phenyl groups towards C_{60} rather than to the metal.

The second reason for choosing TPC lies on its electronic properties. A TPC molecule has a smaller size than C_{60} (20 carbon atoms vs. 60 carbon atoms) and it is not fully conjugated due to the presence of the central sp^3 core. Then, it presents a lower polarizability than a fullerene molecule. It is thus expected a change in the HOMO-LUMO bandgap observed by STS when C_{60} is substituted by TPC.

Co-deposition with C_{60} at different surface temperatures leads to several self-assembled patterns that exhibit different electronic properties, which are explained in the following sections.

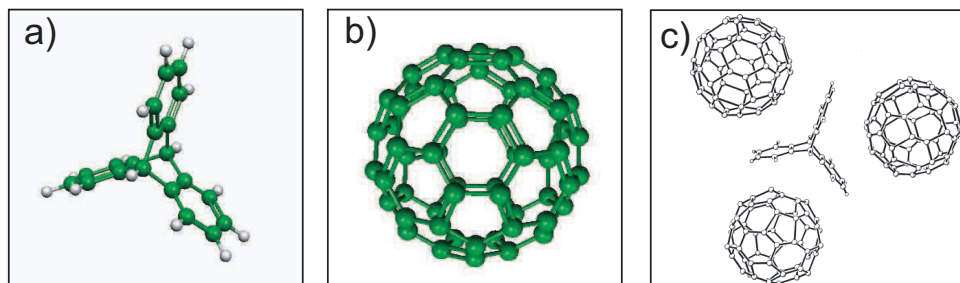


Figure 4.3: (a) Structural model of TPC. (b) Structural model of C_{60} . Green spheres represent C atoms. (c) Inclusion complex found in the bulk structure [10]

4.1.1 Screening in two-dimensional C_{60} /TPC inclusion complexes

Co-deposition of TPC and C_{60} at a surface temperature below 80 K and posterior annealing at 300 K results in the formation of a mixed two-dimensional supramolecular structure (Fig. 4.4(a)). For approximately a TPC/ C_{60} ratio of 1:3, a characteristic mixed domain is formed as shown in Fig. 4.4(b). In this phase, TPC binds preferentially to C_{60} through $\pi - \pi$ interactions forming an inclusion complex, similar to the bulk, and adsorbed parallel to the underlying surface. The bright protrusions correspond to the C_{60} molecules, identified by their characteristic LUMO shape, and the dark rotor-shape depressions correspond to TPC molecules, oriented with the three-fold symmetry axis perpendicular to the surface. Fig. 4.4(c) sketches the typical unit cell of this mixed structure, configured by one TPC molecule per three C_{60} molecules.

The large mobility of TPC on Au(111) restricts the formation of this mixed phase structure based on inclusion complexes only to a small range of surface temperatures and molecular ratios. Surface annealing above 320 K results in a complete segregation of both molecular groups in independent self-assembled domains, where C_{60} molecules nucleate in their characteristic hexagonal phase, and TPC molecules self-assemble in the three-dimensional structure, previously reported.

Upon interaction with TPC in the inclusion complex, C_{60} shows preferred orientations on the Au(111) surface. They correspond to the symmetry axes C3 and C2 as it can be inferred from the images with molecular orbital resolution presented in Fig. 4.5(a). Such preferential adsorption symmetry reveals that the electronic coupling between both hydrocarbons is, although of non-covalent nature, strong enough in order to break the expected random orientation of the fullerene cage adsorbed on Au(111).

The interaction between TPC and C_{60} reveals an upwards shift of ~ 300 meV of the fullerene LUMO with respect to the value of C_{60} embedded in a pure island (Fig. 4.5(b),(c)). Since TPC exhibits a lower polarizability than C_{60} , we can attribute this shift to the substitution of two neighboring fullerenes by two TPC molecules, interacting via H- π and π - π connections with the C_{60} molecule.

Another property of the LUMO resonance, its lineshape, appears to be related to the orientation of the fullerene cage on the surface. Fullerene molecules with a three-fold symmetry axes perpendicular to the Au(111) surface (C3) present a symmetric

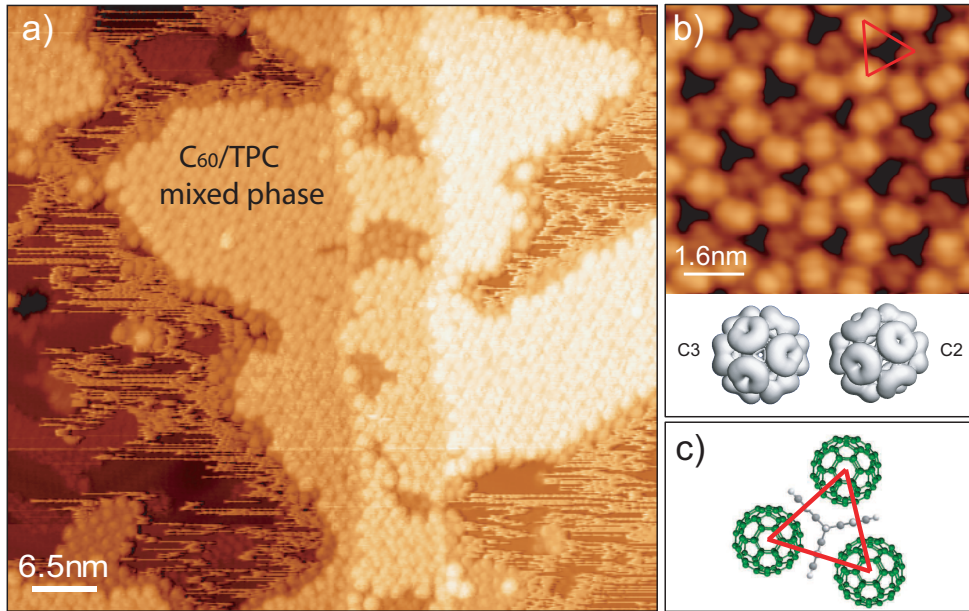


Figure 4.4: (a) Large STM image showing several islands of mixed C_{60} /TPC domains after co-deposition at a sample temperature of 80 K and consequent annealing at 300 K ($V = 2$ V, $I = 0.2$ nA). Extra TPC molecules nucleate at the border of the island and are easily dragged by the STM tip (horizontal lines). (b) Zoom in an ordered structure of TPC/ C_{60} . Each TPC is surrounded by three fullerenes, being the structure stabilized by $\pi - \pi$ interactions. Only two molecular orientations are present, C2 and C3. The red triangle indicates the basic unit cell with its structural model in (c).

LUMO lineshape with a FWHM ~ 0.5 eV (Fig. 4.5(b)). In the case of C_{60} oriented along a C2 symmetry axis, i.e. facing two hexagons towards the surface, the LUMO appears split and broader (Fig. 4.5(c)). The main peak remains at the same energy as in the C3 case, i.e., ~ 1 eV, but a lower shoulder arises at energies ~ 1.2 eV. The FWHM of the main peak amounts to ~ 0.55 eV, as we could obtain by fitting the resonance with various Gaussian functions.

The origin of such correlation between lineshape and orientation of the molecular cage is associated with the different way in which the three-degenerated LUMO resonance is lifted on the surface for each orientation. The adsorption of C_{60} on the surface induces a small deformation of the molecular cage. This distortion breaks the spherical symmetry of the fullerene molecule differently for each orientation and the energy degeneration of the LUMO level breaks down [99].

Excess of C_{60} leads to the coexistence of both pure fullerene islands and mixed C_{60} -TPC regions (Fig. 4.6(a)). In this case, the basic building block (defined by the red triangle in Fig. 4.4(b)) is not ubiquitous in the island and phases with different C_{60} /TPC ratio appear. These inhomogeneous mixed islands offer the possibility to further study the role of the molecular level alignment on C_{60} with a variety of neighbors.

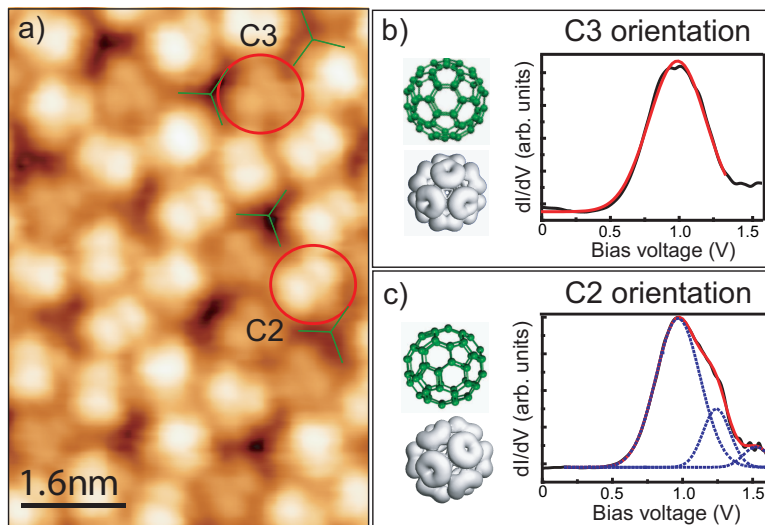


Figure 4.5: (a) STM image with internal resolution of the LUMO C3 and C2 adsorption symmetries ($V = 2$ V, $I = 0.12$ nA). Red circles enclose one example of each molecular orientation. Relative orientation of TPC molecules (green lines) with respect to C_{60} molecules is given. (b) STS taken on a C3-shape fullerene molecule ($V = 2$ V, $I = 1.1$ nA, $V_{ac} = 7 V_{rms}$). The LUMO peak located at ~ 1 eV, can be fitted to a single gaussian curve. (c) STS taken on a C2-shape fullerene molecule ($V = 2$ V, $I = 1.1$ nA, $V_{ac} = 7 V_{rms}$). The LUMO splits and broadens. The resulting curve is fitted by several gaussian curves marked by the blue-dot lines. The spectra are accompanied by a top view of the molecular structure in each orientation and the corresponding LUMO isosurface [98].

In particular we find a gradual shift of the LUMO as the number of fullerene neighbors decrease and are substituted by TPC molecules (Fig. 4.6(b)). A LUMO shift of ~ 80 meV with respect to the value of C_{60} embedded in a pure island is found for a C_{60} surrounded by five fullerenes and a TPC pointing to the C_{60} cage in a H- π fashion (point 2 in Fig. 4.6(b)). According to the estimations of screening energy obtained in Sec. 4.0.2, this shift corresponds basically to the removal of a fullerene. Thus, the shift can only be attributed to the lower number of C_{60} neighbors and the TPC oriented in the H- π fashion towards the probe C_{60} does not have any appreciable screening role. C_{60} marked with the dot 3 has four fullerene neighbors and two TPC, one oriented like in the previous case and another facing the π moieties towards the fullerene cage. In this case the LUMO shift obtained is smaller, amounting only 30 meV. We associate this inferior shift to the additional screening of the TPC molecule enclosing the C_{60} cage with the phenyl moieties. Due to the delocalization of the charge, the polarizability of the TPC is expected to be larger at the aromatic phenyls. Thus, this $\pi - \pi$ interaction between the fullerene and the TPC molecules partially compensates the removal of the neighboring fullerene. Further decrease of the number of neighboring molecules by insertions of TPC in the latter orientation yields an additional shift of the LUMO by 20 meV (graph 4 in Fig. 4.6(b)), similar to the shift obtained in point 3. This

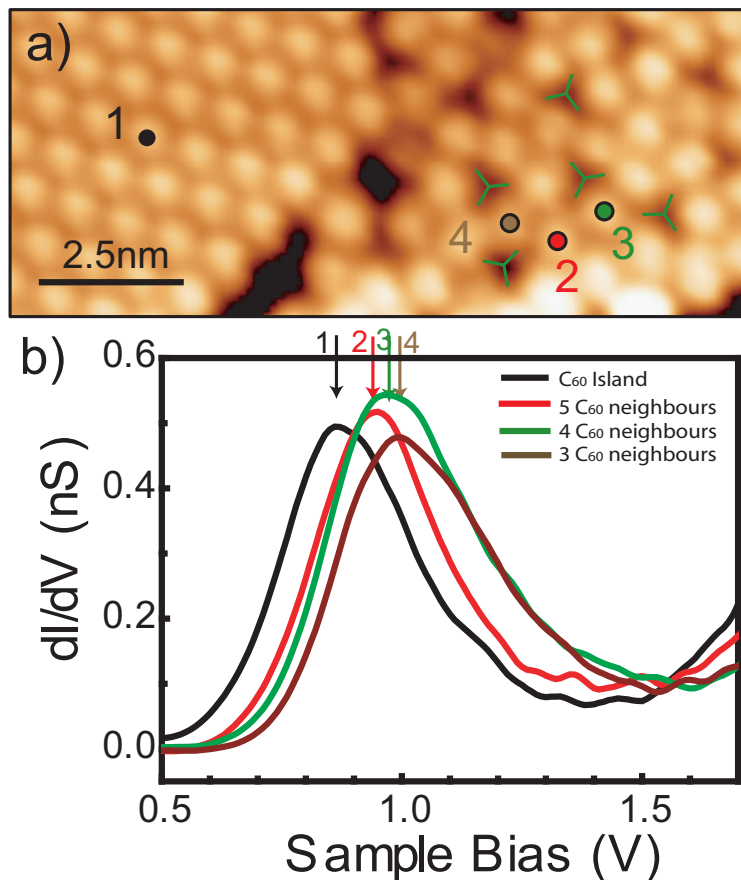


Figure 4.6: (a) Mixed C_{60} -TPC phase obtained with excess of C_{60} . Pure fullerene islands coexist with non-stoichiometric domains of TPC and C_{60} . (b) STS characteristics taken on C_{60} molecules with different molecular environment ($V_{ac} = 6 \text{ mV}_{rms}$, $V = 2.5 \text{ V}$, $I = 1.2 \text{ nA}$). The decrease of fullerene neighbors results in an upward shift of C_{60} LUMO.

results confirm that the resonances observed with STS depend critically on the 'local' polarizability of the neighboring molecules.

4.1.2 C_{60} /TPC Clusters

Interesting molecular nanostructures are found as well when low quantities of C_{60} are co-deposited with TPC on a cold ($\sim 80 \text{ K}$) Au(111) surface without the posterior annealing at room temperature. At this temperature, C_{60} molecules do not diffuse on the surface and they act as nucleation centers for TPC molecules, which diffuse due to their weaker adsorption on Au(111). Fig. 4.7(a) shows the result of this co-deposition. The bright and round features correspond to individual C_{60} molecules. Three fullerene molecules appear surrounded by lower features that are associated to self-assembled TPC in a disordered fashion. The apparent height of the C_{60} molecules

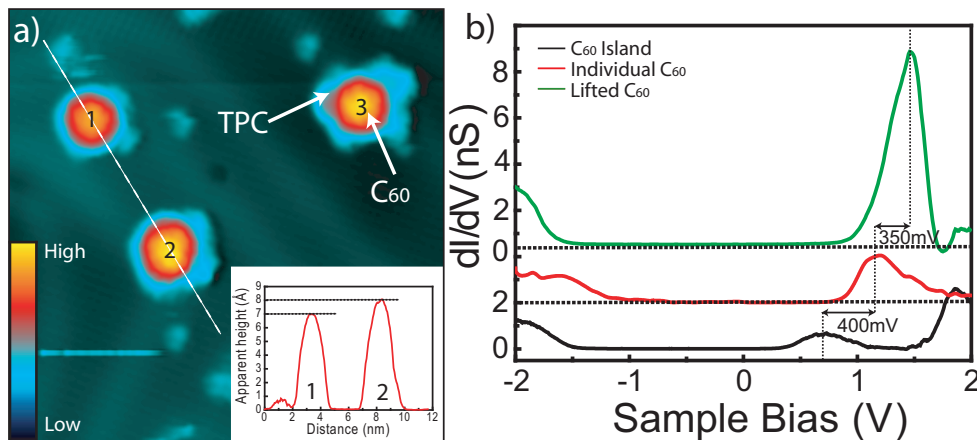


Figure 4.7: (a) STM image ($I = 0.17$ nA, $V = 2$ V) of a low coverage co-deposition of TPC and C_{60} at a surface temperature of 80 K. The scan profile (inset) shows the different apparent height of C_{60} molecules 1 and 2. (b) STS ($I = 3.1$ nA, $V = 2$ V, $V_{ac} = 10$ mV_{rms}) performed on a high C_{60} molecule (green curve) shows an increase on the HOMO-LUMO gap compared to single C_{60} (red) and C_{60} islands (black).

varies depending on the cluster. In Fig. 4.7(a) molecules 2 and 3 appear 1 Å higher than molecule 1 (see inset of Fig. 4.7(a)), which shows the standard apparent height of ~ 7 Å observed for C_{60} adsorbed on Au(111).

The origin of this height increase can have either geometrical or electronic reasons. Regarding the second option, charge transfer between TPC and C_{60} could lead to differences in apparent height. However, the acceptor character of C_{60} in the presence of TPC [10] would induce the opposite effect. C_{60} would have excess of negative charge and its apparent height would decrease. Therefore, we associate the height increase to a physical lifting of the molecular cage from the metal surface.

STS measurements taken on the high fullerene molecules seem to corroborate the lifting hypothesis. The dI/dV spectrum of Fig. 4.7(b) shows a new location of the LUMO resonance at 1.45 eV, i.e., shifted 350 meV upwards in energy compared to the case of the isolated fullerene presented in Fig. 4.1. The upward shift can not be explained by screening, since the presence of TPC would shift, due to its molecular polarizability, the LUMO to lower values than the ones reported in the isolated C_{60} case. Hence, neither screening nor charge transfer can explain the observed LUMO shift. The lifting of the C_{60} cage by the interaction with TPC stands out as a good explanation for the increase of the HOMO-LUMO gap. The larger distance between the molecule and the surface reduces the charge screening by the image charges in the metal. According to this, TPC acts as a thin insulating layer between the metallic surface and the C_{60} molecule. The fullerene molecule is more free-like and the gap opens towards the gas phase value. Furthermore, the linewidth of the LUMO is reduced to ~ 350 meV FWHM, reflecting a longer lifetime of the electron in the resonance. This result agrees with a small decoupling of the C_{60} from the surface due to the interaction with the TPC.

4.2 Conclusions

In this chapter we have studied the change of the HOMO-LUMO gap of a probe C_{60} molecule by the growth and self-organization of several polarizable surroundings formed by C_{60} and the hydrocarbon TPC. Differences in the preparation conditions, such as TPC/ C_{60} ratio and surface temperature during deposition, lead to several self-assembled structures, namely, two-dimensional mixed phases and TPC/ C_{60} clusters.

TPC and C_{60} organize, for an approximate 1:3 ratio, in a two-dimensional mixed phase similar to the bulk structure. Interaction with TPC conditions the C_{60} orientation, revealing a breaking of the LUMO degeneracy for fullerenes adsorbed along the C2 symmetry axes perpendicular to the surface.

Excess of C_{60} leads to the formation of areas with a variety of neighboring conditions, ideal scenario for a study of the screening dependence on molecular environment. The locality of STS allows a direct association of the electronic changes suffered by a single C_{60} to the number of surrounding molecules, their nature, and their relative orientations. In particular, TPC exhibits a lower polarizability than C_{60} . The gradual fullerene substitution by TPC in the mixed molecular arrangement results in a reduction of the charge screening. Furthermore, TPC polarizability exhibits a dependence on its shape: a phenyl ring pointing perpendicular to the C_{60} cage does not reduce significantly the Hubbard energy U , while the $\pi - \pi$ bonding leads to a more significant screening.

Besides screening, the formation of TPC/ C_{60} clusters at low surface temperature leads also to a lifting of the fullerene cage from the surface, that partially decouples the C_{60} molecule from the metal.

